Journal of Ethnopharmacology 363 (2026) 121438

Contents lists available at ScienceDirect

Journal of Ethnopharmacology

journal homepage: www.elsevier.com/locate/jethpharm

# Antiplasmodial and antioxidant constituents from the stem bark of *Haematostaphis barteri* Hook.f. (Anacardiaceae): isolation and bioactivity evaluation

Dé Ndonaï-Koula Lafya Bodeboret Djimtoingar [a], Jean Noël Nyemb [b,*], Hervé Landry Ketsemen [c], Joël Abel Gbaweng Yaya [a], Roméo Feunaing Toko [a], Hinlina Yohanna [a], Samuelson Martin Luther King Boum [a], Céline Hénoumont [d], Sophie Laurent [d], Emmanuel Talla [a,e,**], Marcello Iriti [f,***]

[a] Department of Chemistry, Faculty of Science, The University of Ngaoundere, P.O. Box 454, Ngaoundere, Cameroon
[b] Department of Refining and Petrochemistry, National Advanced School of Mines and Petroleum Industries, The University of Maroua, 08, Kaele, Cameroon
[c] Department of Organic Chemistry, Faculty of Science, The University of Yaounde 1, P.O. Box 812, Yaounde, Cameroon
[d] Department of General Organic and Biomedical Chemistry, Faculty of Medicine and Pharmacy, University of Mons, Belgium
[e] Department of Materials Engeneering, School of Chemical Engeneering and Mineral Industries, University of Ngaoundere, P.O. Box 454, Ngaoundere, Cameroon
[f] Department of Biomedical, Surgical and Dental Sciences, University of Milan, 20129, Milan, Italy

ARTICLE INFO

*Keywords:*
*Haematostaphis barteri*
Antiplasmodial activity
Antioxidant activity
Stigmastane-type steroids
Ellagic acid

ABSTRACT

*Ethnopharmacological relevance: Haematostaphis barteri* Hook.f. (Anacardiaceae) is widely used in African traditional medicine for the management of malaria and other ailments. However, its active antiplasmodial constituents remain insufficiently characterized.

*Aim of the study:* To evaluate the antiplasmodial and antioxidant activities of the stem bark extract of *H. barteri*, identify its major bioactive constituents, and explore their potential interactions with falcipain-2 through exploratory docking studies in order to better understand compounds that may contribute to its traditional medicinal use.

*Materials and methods:* A hydroethanolic stem bark extract was evaluated for *in vitro* antiplasmodial activity against *Plasmodium falciparum* Dd2 (multidrug-resistant) and 3D7 (chloroquine-sensitive) strains. The extract was fractionated by column chromatography into four fractions (A–D), which were similarly tested. Further chromatographic purification of fractions A, B, and C yielded six known compounds: 3-*O*-methylellagic acid-4′-*O*-$\alpha$-rhamnopyranoside (**1**), stigmast-4-en-3,6-dione (**2**), stigmast-3,6-dione (**3**), $\beta$-sitosterol (**4**), 6-hydroxystigmast-4-en-3-one (**5**), and $\beta$-sitosterol-3-O-$\beta$-D-glucoside (**6**). Structures were elucidated using NMR and MS techniques. Exploratory molecular docking was conducted to investigate potential binding modes toward falcipain-2. Antioxidant activity was assessed using DPPH and FRAP assays, and isolated compounds were screened for antiplasmodial activity against both parasite strains.

*Results:* The crude extract exhibited good antiplasmodial activity with $IC_{50}$ values of 13.0 ± 2.0 μg/mL (PfDd2) and 8.6 ± 2.3 μg/mL (Pf3D7). Among the fractions, fraction C showed the highest activity (12.7 ± 0.2 μg/mL; 8.0 ± 1.5 μg/mL), followed by fraction B, A, and D. Six known compounds were isolated, with compounds **1**, **3**, and **5** reported for the first time in the Anacardiaceae family. Docking analysis yielded modest predicted binding energies (−5.4 to −6.8 kcal/mol) and did not show a clear correlation with experimental antiplasmodial activity, suggesting that strong falcipain-2 inhibition is unlikely to represent the primary mechanism of action. All samples demonstrated antioxidant activity, and compound **1** exhibited the strongest effect (DPPH $IC_{50}$ = 59.6 ± 10.4 μg/mL; FRAP $IC_{50}$ = 69.1 ± 0.2 μg/mL). In antiplasmodial assay, the isolated compounds exhibited weak to

* Corresponding author. Department of Refining and Petrochemistry, National Advanced School of Mines and Petroleum Industries, The University of Maroua, P.O. Box 08, Kaele, Cameroon.
** Corresponding author. Department of Chemistry, Faculty of Science, The University of Ngaoundere, P.O. Box 454, Ngaoundere, Cameroon.
*** Corresponding author.
*E-mail addresses:* nyembjeannoel@gmail.com (J.N. Nyemb), Tallae2000@yahoo.fr (E. Talla), marcello.iriti@unimi.it (M. Iriti).

https://doi.org/10.1016/j.jep.2026.121438
Received 4 December 2025; Received in revised form 19 February 2026; Accepted 23 February 2026
Available online 24 February 2026

moderate activity, with compound **1** showing the lowest $IC_{50}$ values among them (31.6 ± 2.9 μM for PfDd2 and 22.1 ± 0.1 μM for Pf3D7).
*Conclusion:* The findings provide preliminary pharmacological support for the traditional antimalarial use of *H. barteri*. *In vitro* assays indicate that several constituents may contribute to the observed inhibition of *Plasmodium* growth, with compound **1** showing moderate activity. Compounds **1**, **3**, and **5** were identified in the Anacardiaceae family for the first time, highlighting their potential as phytochemical markers.

## 1. Introduction

Malaria continues to impose a substantial public health burden worldwide and remains one of the leading causes of illness and death in regions where the disease is common. *Plasmodium falciparum* is responsible for most severe clinical manifestations and fatalities (Ahmed et al., 2024). In 2023, an estimated 263 million malaria cases and over 597,000 deaths occurred globally, with the WHO African Region accounting for nearly 94% of cases and 95% of deaths (WHO, 2024). Despite advances in antimalarial chemotherapy, the rapid spread of resistance, including reduced susceptibility to artemisinin-based combination therapies, underscores the need for novel therapeutic strategies (WHO, 2024).

During infection, *Plasmodium* parasites digest host hemoglobin within erythrocytes, generating redox-active intermediates such as free heme, hydrogen peroxide, and hydroxyl radicals. The accumulation of these reactive species induces oxidative stress, damages erythrocytes, and contributes to inflammation and tissue injury, particularly in the liver and spleen. Oxidative stress has also been implicated in neurological and cognitive complications associated with malaria (Ahmed et al., 2024).

*Haematostaphis barteri* Hook.f. (Anacardiaceae) is a monotypic shrub or small tree native to Africa, occurring on rocky or lateritic soils across several countries including Cameroon (Arbonnier, 2002). In northern Cameroon, traditional healers use its leaves, seeds, bark, and roots, often in combination with other plants or honey, to treat fever, anemia, gastrointestinal disorders, typhoid, and malaria (Roger et al., 2022). Previous studies have reported antioxidant, antiplasmodial, antipyretic, anti-inflammatory, and hepatoprotective activities, with phytochemical analyses revealing terpenoids, flavonoids, tannins, alkaloids, saponins, and reducing sugars (Boampong et al., 2015; Mohammed et al., 2017).

In this study, we report the isolation and structural elucidation of six known compounds from the stem bark of *H. barteri* and evaluate their antioxidant and antiplasmodial activities. Exploratory molecular docking was conducted to assess their potential interactions with the FP2 active site.

## 2. Materials and methods

### 2.1. General experimental procedure

The $^{1}H$ and $^{13}C$ NMR spectra of the isolated compounds were acquired on Bruker spectrometers operating at 500/600 MHz for $^{1}H$ and 125/150 MHz for $^{13}C$ nuclei. Tetramethylsilane (TMS) served as the internal standard. Chemical shifts (δ) are reported in parts per million (ppm), and coupling constants (J) in hertz (Hz). Electrospray ionization mass spectra (ESI-MS) were recorded using an Agilent 6220 time-of-flight (TOF) mass spectrometer. Optical densities for the extracts, fractions, isolated compounds, and reference standards were measured using an APADA V-1100 spectrophotometer. Column chromatography (CC) was carried out on silica gel (200–425 mesh, Merck), and thin-layer chromatography (TLC) employed silica gel $F_{254}$ pre-coated plates (20 × 20 cm, Merck). Compound and fraction spots were initially visualized under UV light at 254 and 365 nm, followed by spraying with 10% $H_2SO_4$ and heating at 102 °C for 3 min. Solvents from extracts and fractions were removed using a Heidolph rotary evaporator.

### 2.2. Plant material

The stem bark of *Haematostaphis barteri* Hook F. were collected in September 2023 at Gouna, a locality near to Garoua in the Northern Region of Cameroon. The plant material was authenticated by Pr. FAWA, a botanist at the University of Ngaoundere, and a voucher specimen was deposited at the National Herbarium of Yaoundé, Cameroon (specimen number 36284/HNC).

### 2.3. Extraction and isolation

The air-dried and ground stem bark of *Haematostaphis barteri* Hook F. (1.5 kg) was macerated at room temperature (~28 °C) with 10 L of an ethanol–water mixture (8:2, v/v) for three consecutive 72-h periods. The combined extracts were concentrated under reduced pressure to afford 49.05 g of crude extract. A portion of this extract (44.22 g) was subjected to open-column chromatography on silica gel, using a gradient of n-hexane– EtOAc (1:0 → 0:1) followed by EtOAc–MeOH (1:0 → 0:1) as the mobile phase. A total of 382 fractions (300 mL each) were collected and subsequently combined into four major fractions (A–D) based on thin-layer chromatography (TLC) profiles.

Fraction A (6.5 g) was further purified by silica gel column chromatography, eluting with n-hexane–EtOAc (100:0 → 85:15), to yield compound **2**. Fraction B (15.1 g) and fraction C (12.92 g) were similarly purified on silica gel columns using n-hexane–EtOAc mixtures (1:0 → 5.5:4.5 for B and 3.5:5.5 → 0:1 for C), resulting in the isolation of compounds **3**, **4**, and **5** from fraction B, and compounds **1** and **6** from fraction C.

### 2.4. Total phenol contents evaluation

The total phenolic content of the extract was determined using a modified Folin–Ciocalteu (FC) assay, following the procedure described by Hatami et al. (2014). Stock solutions of gallic acid (0.02–0.16 mg/mL) and the plant extract (0.02–0.15 mg/mL) were prepared. For each assay, 100 μL of gallic acid standard or extract solution was mixed with 500 μL of FC reagent and 400 μL of 7.5% sodium carbonate ($Na_2CO_3$). The reaction mixtures were incubated at room temperature for 10 min, and the absorbance was measured at 730 nm using a spectrophotometer. The total phenolic content was calculated from a gallic acid calibration curve and expressed as milligrams of gallic acid equivalent per gram of extract (mg GAE/g). The TPC was determined according to the following formula:

$$T = C\ V/m$$

Where, T = total phenolic content mg GAE/g dry extract, C = concentration of gallic acid obtained from calibration curve in mg/mL, V = volume of extract in mL, m = mass of extract in g.

### 2.5. DPPH antiradical scavenging assay

The free radical scavenging activity of the hydroethanolic crude extract, fractions, and isolated compounds was evaluated using the 1,1-diphenyl-2-picrylhydrazyl (DPPH) assay, a widely used method for assessing the antioxidant potential of natural products (Dieng et al., 2017). This assay provides a rapid and reproducible estimate of a compound's ability to neutralize free radicals, which is often associated

with additional biological effects such as anti-inflammatory, cytoprotective, antiplasmodial, and chemopreventive activities.

A 0.04 mg/mL DPPH working solution was prepared by dissolving 4 mg of DPPH in 100 mL of methanol, with the solution protected from light to prevent degradation. Stock solutions of the crude extract, fractions, isolated compounds, and ascorbic acid (positive control) were prepared in methanol at 1 mg/mL. Serial dilutions were then made to obtain final concentrations of 0.25, 0.125, 0.0625, and 0.03125 mg/mL. For each concentration, 0.1 mL of sample solution was combined with 1.9 mL of DPPH solution in a quartz cuvette and incubated in the dark at room temperature (25 ± 2 °C) for 30 min to allow complete interaction between antioxidants and free radicals. The absorbance of each solution was measured at 517 nm using a UV–Visible spectrophotometer, with methanol serving as the blank. All experiments were performed in triplicate and the entire experiment was independently repeated three times to ensure reproducibility. The half-maximal inhibitory concentration ($IC_{50}$), representing the concentration required to scavenge 50% of the DPPH radicals, was calculated using nonlinear regression analysis in Statgraphics Plus version 5.0. Lower $IC_{50}$ values correspond to higher radical scavenging activity. The percentage of radical inhibition was determined using the following equation:

Scavenging effect % = [1 (A of sample)/A of control]

### 2.6. Ferric reducing antioxidant power (FRAP) assay

The ferric-reducing antioxidant power (FRAP) of the extracts, fractions, and isolated compounds was evaluated following the method described by Dieng et al. (2017). In brief, 0.2 mL of each sample at different concentrations was mixed with 0.5 mL of 0.2 M phosphate buffer (pH 6.6) and 0.5 mL of 1% potassium ferricyanide [$K_3Fe(CN)_6$]. The mixtures were incubated at 50 °C for 30 min, after which 0.5 mL of 10% trichloroacetic acid ($CCl_3COOH$) was added. The solutions were centrifuged at 3000 rpm for 10 min, and 1 mL of the resulting supernatant was collected. This supernatant was then combined with 0.2 mL of 0.1% ferric chloride ($FeCl_3$) solution and kept in the dark at room temperature for 30 min. The absorbance was measured at 700 nm using a UV–Visible spectrophotometer. The antioxidant activity, reflecting the electron-donating ability of the samples, was expressed as the reducing power (RP) according to the following equation:

$$RP = 100\ (A_a\text{-}A_b)\ /A_a$$

Where $A_a$ is the absorbance of the extract and Ab is the absorbance of the blank.

### 2.7. In vitro inhibition of Plasmodium falciparum

The chloroquine-sensitive (3D7) and multidrug-resistant (Dd2) strains of *Plasmodium falciparum* were sourced from the Biodefense and Emerging Infections (BEI) Research Resources, Manassas, VA, USA. Parasites were cultured and maintained following a modified version of the method described by Trager and Jensen (1976).

#### 2.7.1. Parasite's culture and maintenance

The chloroquine-sensitive (Pf3D7, MRA-102) and multidrug-resistant (PfDd2, MRA-150) strains of *Plasmodium falciparum* were cultured in freshly obtained $O^+$ human erythrocytes at 4% hematocrit using complete RPMI 1640 medium. The medium was prepared by supplementing 500 mL of RPMI 1640 (Gibco, UK) with 25 mM HEPES (Gibco, UK), 0.5% Albumax I (Gibco, USA), 1X hypoxanthine (Gibco, USA), and 50 μg/mL gentamicin (Gibco, China). Cultures were maintained at 37 °C in a humidified incubator under 5% $CO_2$, with the medium replaced daily to support parasite growth. Thin blood smears were prepared, Giemsa-stained, and examined under oil immersion microscopy to track parasitemia and parasite development. Synchronized ring-stage parasites were obtained two days prior to each assay by serial treatment with 5% D-sorbitol, following the method of Lambros and Vanderberg (1979).

#### 2.7.2. SYBR Green fluorescence-based assay

Drug sensitivity was assessed using a SYBR Green I fluorescence assay in 96-well microplates, following the procedure described by Smilkstein et al. (2004). This assay relies on the selective fluorescence of SYBR Green in the presence of parasite DNA, enabling specific monitoring of *Plasmodium falciparum* growth within enucleated human red blood cells.

Sorbitol-synchronized ring-stage parasites (1% hematocrit, 2% parasitemia) were incubated in 96-well plates with 10 μL of pre-diluted plant extracts, isolated compounds, or reference drugs added to 90 μL of culture under standard conditions at 37 °C for 72 h. After incubation, 100 μL of SYBR Green I lysis buffer was added to each well. The buffer was prepared by combining 6 μL of 10,000 × SYBR Green I (Invitrogen), 600 μL of RBC lysis buffer (25 mM Tris, pH 7.5), 360 μL of 7.5 mM EDTA, 19.2 μL of 0.012% saponin solution, and 28.8 μL of 0.08% Triton X-100. Plates were incubated in the dark at 37 °C for 1 h, after which fluorescence was recorded using a TECAN Infinite M200 microplate reader at excitation and emission wavelengths of 485 nm and 538 nm, respectively.

### 2.8. Molecular docking analysis of isolated compounds against Falcipain-2

Molecular docking was performed to investigate potential interactions between the isolated compounds and FP2 (PDB ID: 3BPF) using AutoDock Vina v1.2.7 (Singh et al., 2022).

#### 2.8.1. Preparation of ligands

Three-dimensional structures of the isolated compounds were generated with Chem3D 15.0, exported in.pdb format, and subjected to energy minimization to optimize geometry and reduce steric strain.

#### 2.8.2. Preparation of protein targets

The X-ray structure of FP2 complexed with E64 (PDB ID: 3BPF) was retrieved from the Protein Data Bank. Crystallographic water molecules, ions, and bound ligands were removed, polar hydrogens were added, and Gasteiger and Kollman charges were assigned using AutoDockTools. The protein structure was energy-minimized prior to docking.

#### 2.8.3. Docking procedure

The docking grid was centered on the FP2 active site, encompassing the catalytic region at coordinates X = −57.907, Y = −1.465, and Z = −16.025. Each ligand underwent fifteen independent docking runs, and the conformation with the lowest binding free energy was selected for analysis. Protein–ligand interactions were visualized and examined using Discovery Studio Visualizer.

### 2.9. Statistical analysis

All data analyses were conducted using GraphPad Prism version 5.0. The bioassays were performed in triplicate and the entire experiment was independently repeated three times to ensure reproducibility. For comparisons involving three or more groups with a single independent variable, one-way ANOVA was applied, followed by Newman-Keuls post-hoc test for multiple comparisons. Differences were considered statistically significant at $p < 0.05$.

## 3. Results and discussion

### 3.1. Isolation and characterization of compounds

The most active fractions (A, B, and C) obtained from the crude hydroethanolic extract of the stem bark of *Haematostaphis barteri* Hook. f., were further purified through successive silica gel column chromatography (CC). This process yielded six known compounds: 3-*O*-methylellagic acid-4′-*O*-*α*-rhamnopyranoside (**1**) (Djoukeng et al., 2007); stigmast-4-en-3,6-dione (**2**) (Wei et al., 2004); stigmastane-3,6-dione (**3**) (Wei et al., 2004); *β*-sitosterol (**4**) (Nyemb et al., 2018); 6-hydroxystigmast-4-en-3-one (**5**) (Liu et al., 2023); and *β*-sitosterol-3-*O*-*β*-D-glucoside (**6**) (Adekunle et al., 2025) (Fig. 1). The identification of these constituents was achieved through detailed interpretation of their spectroscopic and mass spectrometric data, followed by comparison with reported literature values. To our knowledge, this represents the first structural characterization of phytochemical constituents isolated from *H. barteri*.

*3-O-methylellagic acid-4′-O-α-rhamnopyranoside* (**1**): yellow needle; m.p.: 358-359 °C; $[\alpha]_D^{25}$ = -18.2° (*c* 0.80, DMSO); ES (−): m/z 461 [M-H]$^-$, m/z 315 [M-H-rhamnose]$^-$ corresponding to the formula $C_{21}H_{18}O_{12}$. $^1$H NMR (600 MHz, MeOD): $\delta_H$ 7.63 (1H, s, H-5), 7.63 (1H, s, H-5′), 5.58 (1H, d, H-1′), 7.63 (1H, S, H-5″), 1.33 (3H, H-6″), 4.03 (3H, S, $OCH_3$).$^{13}$C NMR (150 MHz, MeOD): $\delta_C$ 113.4 (C-1), 127.6 (C-2), 140.4 (C-3), 152.6 (C-4), 112.4 (C-5), 100.2 (C-6), 159.6 (C-7), 114.8 (C-1′), 136.6 (C-2′), 141.7 (C-3′), 146.9 (C-4′), 111.7 (C-5), 111.5 (C-6′), 159.5 (C-7′), 100.2 (C-1″), 69.8 (C-2″), 70.6 (C-3″), 72.3 (C-4″), 70.3 (C-5″), 16.6 (C-6″), 60.6 ($OCH_3$) (Djoukeng et al., 2007).

*Stigmast-4-en-3,6-dione* (**2**): Yellow solid compound; m.p.: 162–163 °C; $[\alpha]_D^{24}$ = - 38.2° (*c* 0.24, $CHCl_3$); ES (+): m/z 427.84 [M-H]$^+$, $^1$H NMR (600 MHz, $CDCl_3$): $\delta_H$ 6.19 (1H, S, H-4), 2.13 (t, 2H, *J* = 3.96 Hz, H-2), 2.69 (dd, Ha, Hb, $J_a = J_b$ = 4.02 Hz, $J_{ab}$ = 16.98 Hz), 0.74 (3H, s, H-18), 1.18 (3H, s, H-19), 0,96 (3H, d, *J* = 6.54 Hz, H-21), 0.84 (3H, d, *J* = 6.54 Hz), 0.85 (3H, s, H-27), 0.87 (d, 3H, *J* = 2.58 Hz, H-29). $^{13}$C NMR (150 MHz, $CDCl_3$): 35.5 (C-1), 33.9 (C-2), 199.5 (C-3), 125.4 (C-4), 161.0 (C-5), 202.3 (C-6), 46.8 (C-7), 34.2 (C-8), 50.9 (C-9), 39. 8 (C-10), 20.8(C-11), 39.1 (C-12), 42.5 (C-13), 56.5 (C-14), 23.9 (C-15), 28.0 (C-16), 55.8 (C-17), 11.9 (C-18), 17.5 (C-19), 36.0 (C-20), 18.7 (C-21), 33.8 (C-22), 26.0 (C-23), 45.8 (C-24), 29.1 (C-25), 19.0 (C-26), 19.8 (C-27), 23.0 (C-28), 11.9 (C-29) (Pardo et al., 2000).

*Stigmast-3,6-dione* (**3**): White powder; m.p. 196-197 °C; $[\alpha]_D^{25}$ = + 26.7° (*c* 0.19, $CHCl_3$); $^1$H NMR (Acetone-$d_6$, 126 MHz): $\delta_H$ 0.77 (3H, s, H-18), 1.00 (3H, s, H-19), 0.89 (3H, d, H-21), 0.87 (3H, d, H-26), 0.85 (3H, d, H-27), 0.86 (3H, d, H-29).$^{13}$CNMR (Acetone-$d_6$, 126 MHz): $\delta_C$ 58.6 (C-1), 37.8 (C-2), 210.3 (C-3), 37.6 (C-4), 57.7 (C-5), 209.0 (C-6), 46.9 (C-7), 38.6 (C-8), 53.9 (C-9), 41.3 (C-10), 22.3 (C-11), 40.4 (C-12), 43.7 (C-13), 57.5 (C-14), 24.7 (C-15), 28.8 (C-16), 56.8 (C-17), 12.3 (C-18), 12.6 (C-19), 36.9 (C-20), 19.6 (C-21), 34.66 (C-22), 26.8 (C-23), 46.7 (C-24), 28.8 (C-25), 20.1 (C-26), 19.3 (C-27), 23.7 (C-28), 12.6 (C-29) (Wei et al., 2004).

*β-sitosterol* (**4**)*:* White powder; m.p. 139-110 °C; $[\alpha]_D^{25}$ = −37.0° (*c* 0.1, $CHCl_3$); $^1$H NMR ($CDCl_3$, 600 MHz): $\delta_H$ 5.29 (1H, m, H-6), 3.45 (1H, m, H-3), 1.05 (3H, s, H-19), 0,98 (3H, d, *J* = 6.3 Hz), 0.89 (3H, d, *J* = 3.05 Hz, H-26), 0.87 (3H, d, *J* = 2.3 Hz, H-27), 0.86 (3H, s, H-29), 0.75 (3H, s, H-18). $^{13}$C NMR ($CDCl_3$, 126 MHz): $\delta_C$ 140.7 (C-5), 121.7 (C-6), 71.8 (C-3), 56.8 (C-14), 56.1 (C-17), 50.1 (C-9), 50.1 (C-24), 42.3 (C-13), 42.3 (C-4), 39.6 (C-12), 37.2 (C-1), 36.5 (C-10), 39.6 (C-20), 33.9 (C-22), 32.1 (C-7), 31.8 (C-8), 31.8 (C-2), 29.1 (C-25), 28.2(C-16), 26.0 (C-23), 24.3 (C-15), 26.8 (C-28), 21.7 (C-11), 19.0 (C-26), 19.4 (C-19), 21.2 (C-27), 21.0 (C-21), 11.8 (C-29), 12.0 (C-18) (Madeleine et al., 2020; Mahamat et al., 2021; Munvera et al., 2021; Nyemb et al., 2018).

*6β-hydroxystigmast-4-en-3-one* (**5**)*:* White needle; m.p. 207-208 °C; $[\alpha]_D^{25}$ = +30.2° (*c* 0.15, $CHCl_3$); ES (+): m/z 452 [M-H]$^+$ corresponding to the formula $C_{29}H_{48}O_2$. $^1$H NMR (500 MHz, $CDCl_3$): 5.80 (1H, s, H-4), 4.34 (1H, d, *J* = 5.0 Hz, H-6), 0.77 (3H, s, H-18), 1.39 (3H, s, H-19), 0.95 (3H, d, *J* = 6.6 Hz, H-21), 0.89 (3H, d, *J* = 5.0 Hz, H-27), 0.81 (3H, d, *J* = 5.2 Hz, H-26) 0.86 (3H, t, *J* = 7.0 Hz, H-29).$^{13}$C NMR (125 MHz, $CDCl_3$): 37.1 (C-1), 34.3 (C-2), 200.4 (C-3), 126.6 (C-4), 168.5 (C-5); 73.3 (C-6), 38.6 (C-7), 29.7 (C-8), 53.7 (C-9), 38.0 (C-10), 21.0 (C-11), 39.6 (C-12), 42.5 (C-13), 56.1 (C-14), 24.2 (C-15), 28.2 (C-16), 55.9 (C-

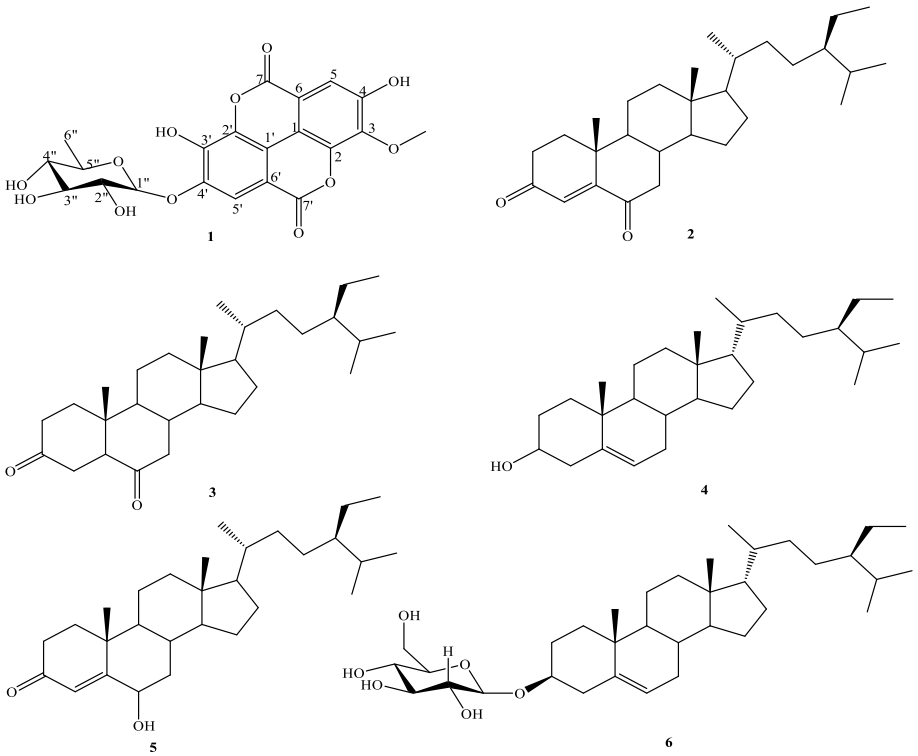


**Fig. 1.** Compounds isolated from the stem bark of *H. barteri* Hook.f. f the isolated compoun

17), 12.0 (C-18), 19.5 (C-19), 36.1 (C-20), 18.7 (C-21), 33.9 (C-22),26.0 (C-23), 45.8 (C-24), 29.1 (C-25), 19.8 (C-26), 19.0 (C-27), 23.4 (C-28), 12.0 (C-29) (Liu et al., 2023).

*β-sitosterol-3-O-β-D-glucoside* (**6**)*:* White powder; m.p. 284-285 °C; $[\alpha]_D^{20} = -29.0°$ (*c* 0.1, Pyr.); $^1$H NMR ($CDCl_3$, 600 MHz): $\delta_H$ 5.29 (1H, m, H-6), 3.45 (1H, m, H-3), 1.05 (3H, s, H-19), 0,98 (3H, d, $J = 6.3$ Hz), 0.89 (3H, d, $J = 3.05$ Hz, H-26), 0.87 (3H, d, $J = 2.3$ Hz, H-27), 0.86 (3H, s, H-29), 0.75 (3H, s, H-18).$^{13}$C NMR ($CDCl_3$, 126 MHz): $\delta_C$ 140.7 (C-5), 121.7 (C-6), 71.8 (C-3), 56.8 (C-14), 56.1 (C-17), 50.1 (C-9), 50.1 (C-24), 42.3 (C-13), 42.3 (C-4), 39.6 (C-12), 37.2 (C-1), 36.5 (C-10), 39.6 (C-20), 33.9 (C-22), 32.1 (C-7), 31.8 (C-8), 31.8 (C-2), 29.1 (C-25), 28.2 (C-16), 26.0 (C-23), 24.3 (C-15), 26.8 (C-28), 21.7 (C-11), 19.0 (C-26), 19.4 (C-19), 21.2 (C-27), 21.0 (C-21), 11.8 (C-29), 12.0 (C-18) (Abdou et al., 2022; Munvera et al., 2021; Adekunle et al., 2025).

To the best of our knowledge, this study represents the first isolation and structural characterization of compounds **1**–**6** from the genus *Haematostaphis* and specifically from *H. barteri*. The isolated metabolites fall into two major chemical groups: sterols (**2**–**6**) and a phenolic acid derivative (**1**), both of which are well documented within the Anacardiaceae (Mitchell et al., 2022; Schulze-Kaysers et al., 2015). Notably, compounds **4** and **6** have been previously reported from the stem bark of *Anacardium occidentale* L. and *Lannea kerstingii* Engl. & K. Krause (Iheanacho et al., 2024; Njinga et al., 2016), while compound **2** and a structural isomer of compound **3** were earlier obtained from the root bark of *Lannea antiscorbutica* (Hiern) Engl. (Mvingu et al., 2025). Compounds **1**, **3**, and **5** are to the best of our knowledge, reported here for the first time within the Anacardiaceae family. Although *Haematostaphis* has not yet been included in molecular phylogenetic analyses (Mitchell et al., 2022), these preliminary phytochemical observations may provide useful insights into its affinities within the family. In particular, compounds **1**, **3**, and **5** could potentially serve as tentative chemotaxonomic markers in future systematic studies involving Anacardiaceae taxa, though additional investigations and a broader set of metabolites are required to confirm their relevance.

### 3.2. Total phenolic content and antioxidant results

The hydroethanolic extract exhibited a total phenolic content (TPC) of 18.56 ± 3.86 mg GAE/g, reflecting a moderate level of phenolic constituents. Phenolics constitute one of the major groups of secondary metabolites in plants and are well known for their antioxidant potential, which arises from their ability to donate electrons or hydrogen atoms and their capacity to chelate transition metals (Rice-Evans et al., 1997). The moderate TPC measured in this study is consistent with the antiradical effects demonstrated in the DPPH and FRAP assays.

The antioxidant capacities of the extract and its fractions, evaluated using the DPPH free radical scavenging and Ferric-Reducing Antioxidant Power (FRAP) assays, are presented in Table 1. Based on the activity scale proposed by —Talla et al. (2016)good ($IC_{50} < 69$ μg/mL), moderate ($IC_{50} < 161$ μg/mL), and low ($IC_{50} > 161$ μg/mL)—the hydroethanolic crude extract and several fractions exhibited good to moderate reducing power in the FRAP assay, while all samples showed low activity in the DPPH assay. The crude extract demonstrated notable ferric-reducing capacity ($IC_{50} = 55.2 \pm 2.3$ μg/mL) but only weak DPPH scavenging ability ($IC_{50} = 262.1 \pm 3.2$ μg/mL). Among the fractions, fraction C displayed the strongest FRAP activity ($IC_{50} = 6.5 \pm 0.6$ μg/mL), followed sequentially by fractions D, B, and A. In contrast, all fractions showed limited scavenging of the DPPH radical, indicating that their antioxidant potential is more strongly expressed through reducing mechanisms than hydrogen-donating activity.

Notably, 3-*O*-methylellagic acid-4′-*O*-*α*-rhamnopyranoside (**1**), isolated from fraction C, exhibited the highest antioxidant activity among the isolated constituents in both assays, with $IC_{50}$ values of 69.1 ± 0.2 μg/mL (DPPH) and 59.6 ± 10.4 μg/mL (FRAP). The comparable effectiveness of compound **1** across the two methods likely reflects its phenolic framework, since phenolic metabolites are known for their redox properties, enabling them to donate electrons or hydrogen atoms, chelate metals, and neutralize reactive oxygen species (Talla et al., 2016). This compound may therefore contribute significantly to the overall antioxidant profile of the crude extract. Compound **2** exhibited moderate ferric-reducing activity (FRAP $IC_{50} = 149.1 \pm 1.9$ μg/mL) and showed good radical-scavenging potential in the DPPH assay ($IC_{50} = 60.7 \pm 11.1$ μg/mL). In contrast, compound **3** demonstrated low activity in the DPPH assay but displayed good reducing power in the FRAP assay ($IC_{50} = 81.5 \pm 1.1$ μg/mL). Compound **4** presented moderate antioxidant capacity in the DPPH test, while its performance in the FRAP assay was low, suggesting limited reducing ability. The intermediate antioxidant activities observed for these compounds likely reflect structural differences such as patterns of substitution, functional groups, and degrees of saturation that can influence radical-scavenging behavior by altering electron delocalization or the ability to donate protons (Heim et al., 2002). In contrast, compounds **5** and **6** showed low activity in both assays, which may be attributed to limited redox capacity or steric factors that hinder effective interaction with the radicals.

**Table 1**
Radical scavenging activity (DPPH assay), and reducing activity (FRAP assay) of hydro-ethanolic extract and isolated compounds from *H. barteri*.

| Sample | $IC_{50}$ (μg/mL) | |
|---|---|---|
| | DPPH | FRAP |
| Hydro-ethanolic Extract | $262.1 \pm 3.2^a$ | $55.2 \pm 2.3^a$ |
| Fraction A | $214 \pm 1.2^b$ | $121.6 \pm 4.0^b$ |
| Fraction B | $351.2 \pm 4.4^c$ | $84.9 \pm 0.8^c$ |
| Fraction C | $190.6 \pm 2.6^d$ | $6.5 \pm 0.6^d$ |
| Fraction D | $418.5 \pm 7.1^e$ | $43.1 \pm 1.3^e$ |
| 3-*O*-methylellagic acid-4′-*O*-*α*-rhamnopyranoside (**1**) | $59.6 \pm 10.4^f$ | $69.1 \pm 0.2^f$ |
| Stigmast-4-en-3,6-dione (**2**) | $60.7 \pm 11.1^f$ | $149.1 \pm 1.9^g$ |
| Stigmast-3,6-dione (**3**) | $208.6 \pm 3.7^b$ | $81.5 \pm 1.1^c$ |
| *β*-sitosterol (**4**) | $159.1 \pm 2.1^g$ | $202.2 \pm 0.9^h$ |
| 6-hydroxystigmast-4-en-3-one (**5**) | $227.3 \pm 2.4^h$ | $222.3 \pm 2.6^i$ |
| *β*-sitosterol-3-*O*-*β*-D-glucoside (**6**) | $207.5 \pm 1.2^b$ | $263.1 \pm 7.7^j$ |
| Ascorbic acid | $1.0 \pm 0.1^i$ | $3.4 \pm 0.7^d$ |

Ascorbic acid was utilized as the reference drug. Data presented as mean values for triplicates ± SD (standard deviation). Mean values followed by the same letter superscripts in a column are not significantly different ($n = 3$, $p < 0.05$). ND: not defined.

The antioxidant profile of the crude extract closely resembles that of compounds **1** and **3**, particularly in the FRAP assay, where its activity surpasses that of the other isolated constituents. This pattern suggests that these two compounds may significantly contribute to the extract's reducing power, while the presence of additional minor metabolites or synergistic interactions may further enhance overall activity. Conversely, in the DPPH assay, the crude extract showed weaker activity than all isolated compounds, indicating a possible antagonistic effect or the dilution of active constituents within the complex extract matrix.

Despite the antioxidant capacities demonstrated by the extract, fractions, and isolated compounds, all samples exhibited markedly lower activity than the reference standard, ascorbic acid, which displayed $IC_{50}$ values of 1.0 ± 0.1 μg/mL (DPPH) and 3.4 ± 0.7 μg/mL (FRAP). Nevertheless, the present findings align with previous reports by Boampong et al. (2015) and Ezekiel et al. (2016), which also documented antioxidant properties in stem bark extracts of *H. barteri*.

### 3.3. In vitro antiplasmodial activity results

The crude hydroethanolic extract, its fractions, and the isolated compounds from *H. barteri* were assessed *in vitro* for their antiplasmodial activity against both chloroquine-sensitive (*Pf* 3D7) and multidrug-resistant (*Pf* Dd2) strains of *Plasmodium falciparum* using a SYBR Green-based fluorescence assay to measure parasite growth inhibition.

In antiplasmodial bioassays, crude extracts and fractions are

typically expressed in μg/mL, whereas pure compounds are reported in μM (or occasionally μg/mL) to reflect molar or mass concentrations accurately (Konyanee et al., 2024). For this study, the activity of isolated compounds was interpreted using the criteria of Batista et al. (2009): $IC_{50} \leq 1$ μM, excellent; $1 < IC_{50} \leq 20$ μM, good; $20 < IC_{50} \leq 100$ μM, moderate; $100 < IC_{50} \leq 200$ μM, low; and $IC_{50} > 200$ μM, inactive. For crude extracts and fractions, classification followed Muganza et al. (2016): pronounced activity, $IC_{50} \leq 5$ μg/mL; good, $5 < IC_{50} \leq 10$ μg/mL; moderate, $10 < IC_{50} \leq 20$ μg/mL; low, $20 < IC_{50} \leq 40$ μg/mL; and inactive, $IC_{50} > 40$ μg/mL. Based on these thresholds, all samples except compound **6** demonstrated good to moderate activity, though their potency was substantially lower than the reference drugs artemisinin and chloroquine (Table 2).

The crude hydroethanolic extract of *H. barteri* stem bark displayed good activity against the chloroquine-sensitive strain (*Pf* 3D7) and moderate activity against the multidrug-resistant strain (*Pf* Dd2), with $IC_{50}$ values of 8.6 ± 2.3 μg/mL and 13.0 ± 2.0 μg/mL, respectively. Among the fractions, fraction C exhibited the highest activity, showing good inhibition of *Pf* Dd2 ($IC_{50}$ = 8.0 ± 1.5 μg/mL) and moderate activity against *Pf* 3D7 ($IC_{50}$ = 12.7 ± 0.2 μg/mL). Fraction B followed closely, with $IC_{50}$ values of 9.3 ± 0.7 μg/mL (*Pf* Dd2) and 11.5 ± 0.0 μg/mL (*Pf* 3D7). Fraction A displayed moderate activity against *Pf* Dd2 ($IC_{50}$ = 19.8 ± 0.2 μg/mL) but only low activity against *Pf* 3D7 ($IC_{50}$ = 34.0 ± 1.6 μg/mL), whereas fraction D was the least potent, showing low activity against *Pf* Dd2 ($IC_{50}$ = 21.1 ± 1.2 μg/mL) and inactivity against *Pf* 3D7 ($IC_{50}$ = 53.71 ± 2.41 μg/mL).

Among the isolated constituents, the phenolic compound 3-*O*-methylellagic acid-4′-*O*-*α*-rhamnopyranoside (**1**), derived from fraction C, demonstrated moderate activity against both strains, with $IC_{50}$ values of 22.1 ± 0.1 μM (*Pf* 3D7) and 31.6 ± 2.9 μM (*Pf* Dd2). Stigmastane-type steroids (compounds **2**–**5**) exhibited moderate to low activity: compound **2** showed the highest activity among them ($IC_{50} \approx 47.5$ μM for both strains), while compounds **3** and **4** had slightly higher $IC_{50}$ values against *Pf* Dd2 compared to *Pf* 3D7. Compound **5** displayed moderate activity against *Pf* 3D7 but low activity against *Pf* Dd2, and compound **6** was inactive against both strains (Table 2).

It should be noted that the superior activity of the crude extract may result not only from potential synergistic interactions among its constituents, but also from minor or as-yet-uncharacterized compounds that could contribute significantly to its antiplasmodial activity. Furthermore, the similarity in activity between the crude extract and fraction C indicates that compound **1** may represent a major contributor to the observed antiplasmodial effect of this fraction. Although the extracts and isolated compounds also exhibited antioxidant activity, the present study does not establish a mechanistic link between antioxidant capacity and parasite growth inhibition. While oxidative stress and reactive oxygen species are known to be involved in malaria pathophysiology (Vasquez et al., 2021), any relationship between antioxidant properties and antiplasmodial effects in this study should be regarded as hypothetical, as no ROS-related assays or mechanistic experiments were performed to evaluate this connection.

**Table 2**
Antiplasmodial activity of compounds, fractions and extracts on *Plasmodium falciparum* strains.

| Samples | *Pf*Dd2 | *Pf*3D7 |
|---|---|---|
| **Extract and fractions** | **$IC_{50}$ (μg/mL)** | |
| Hydro-ethanolic Extract | 13.0 ± 2.0* | 8.6 ± 2.3* |
| Fraction A | 34.0 ± 1.6** | 19.8 ± 0.2** |
| Fraction B | 11.5 ± 0.0* | 9.3 ± 0.7* |
| Fraction C | 12.7 ± 0.2* | 8.0 ± 1.5* |
| Fraction D | 53.7 ± 2.4*** | 21.1 ± 1.2** |
| **Compounds** | **$IC_{50}$ (μM)** | |
| 3-*O*-methylellagic acid-4′-*O*-*α*-rhamnopyranoside (**1**) | 31.6 ± 2.9[a] | 22.1 ± 0.1[a] |
| Stigmast-4-en-3,6-dione (**2**) | 47.5 ± 3.7[b] | 47.6 ± 6.8[b] |
| Stigmast-3,6-dione (**3**) | 53.7 ± 3.4[c] | 46.8 ± 2.7[b] |
| *β*-sitosterol (**4**) | 70.8 ± 4.7[d] | 73.4 ± 3.2[c] |
| 6-hydroxystigmast-4-en-3-one (**5**) | 93.2 ± 0.8[e] | 139.8 ± 2.7[d] |
| *β*-sitosterol-3-*O*-*β*-D-glucoside (**6**) | ND | ND |
| **Art** | 0.03 ± 0.01[f] | 0.04 ± 0.01[e] |
| **CQ** | 0.7 ± 0.1[f] | 0.05 ± 0.01[e] |

Artemisinin (Art) and chloroquine (CQ) were utilized as reference drugs. Data presented as mean values for triplicates ± SD (standard deviation). Mean values followed by the same superscripts in a column are not significantly different ($n = 3$, $p < 0.05$). ND: not defined.

Although no prior data exist for compound **1**, related derivatives provide useful context. For instance, 3,3′,4-tri-*O*-methylellagic acid, lacking a sugar moiety and bearing additional methyl groups, exhibited notable activity ($IC_{50}$ = 1.9 μM) against multidrug-resistant *Pf* Dd2, approximately 18-fold more potent than compound **1**, suggesting that methylation may enhance antiplasmodial potency (Dongmo et al., 2023). Similarly, stigmastane-type steroids have previously shown moderate antiplasmodial activity in the twigs of *Vernonia amygdalina* (Happi et al., 2025) and the stem bark of *Dryobalanops oblongifolia* (Indriani et al., 2020).

The experimental antiplasmodial data reveal clear structure-activity trends. Compound **1**, bearing a methylated ellagic acid core with a rhamnose moiety, exhibited the most potent activity among the isolated constituents, with $IC_{50}$ values of 22.1 ± 0.1 μM against *Pf* 3D7 and 31.6 ± 2.9 μM against *Pf* Dd2. Among the steroid derivatives, compound **2** (stigmast-4-en-5,6-dione, $IC_{50} \approx 47.5$ μM) showed superior activity compared to the saturated analog **3** (stigmast-5,6-dione, $IC_{50} \approx 50$ μM), suggesting that the $\Delta^4$ unsaturation may enhance biological activity. Introduction of a hydroxyl group at C-6, as in compound **5** (6-hydroxystigmast-4-en-3-one), significantly reduced potency, possibly due to altered lipophilicity or membrane permeability. Glycosylation of the steroid nucleus, as observed in compound **6** (*β*-sitosterol-3-*O*-*β*-D-glucoside), resulted in complete loss of activity, likely reflecting poor cellular uptake of this highly polar derivative. These structure-activity observations provide a rational basis for future optimization efforts. Exploratory molecular docking suggested possible interactions with falcipain-2 (Section 3.4); however, the computational predictions showed limited correlation with experimental activity, indicating that the actual mechanism of action requires further investigation through direct enzyme inhibition assays and cellular target identification studies.

It should be noted that the present study did not evaluate cytotoxicity against mammalian cells, selectivity indices, bioavailability, or metabolic stability. These parameters will be the subject of future investigations to further assess the antimalarial potential of the isolated compounds.

### 3.4. Molecular docking results

Molecular docking was performed as a preliminary exploratory approach to investigate the potential molecular mechanisms underlying the observed antiplasmodial activity. Specifically, falcipain-2, a well-established cysteine protease involved in hemoglobin degradation in *Plasmodium falciparum*, was selected as a rational and validated antimalarial target. This analysis aimed to evaluate whether falcipain-2 could represent a plausible molecular target for the isolated compounds.

The predicted binding energies ranged from −5.4 to −6.8 kcal/mol (Table S1). Compound **1** showed the most favorable predicted affinity (−6.8 kcal/mol), while the steroid derivatives exhibited comparable values within a narrow range. The reference inhibitor E64 yielded a docking score of −5.8 kcal/mol under the same non-covalent protocol.

Overall, the predicted affinities were modest and did not show a clear relationship with the experimental antiplasmodial activities. These results suggest that strong inhibition of falcipain-2 is unlikely to be the primary mechanism underlying the observed biological effects.

The docking analysis is therefore presented as a qualitative, hypothesis-generating tool rather than mechanistic evidence. While the compounds appear structurally compatible with occupancy of the

falcipain-2 binding pocket, experimental enzyme inhibition studies would be required to confirm any direct interaction.

## 4. Conclusion

This work represents the first detailed phytochemical and bioactivity assessment of the stem bark of *Haematostaphis barteri*. Six known compounds were isolated and structurally elucidated, comprising one phenolic derivative and five stigmastane-type steroids. The crude extract and the purified compounds exhibited antioxidant and antiplasmodial effects, with 3-*O*-methylellagic acid-4′-*O*-*α*-rhamnopyranoside (**1**) showing the highest activity among the constituents. The enhanced activity observed in the crude extract suggests potential synergistic interactions among the isolated metabolites. An exploratory molecular docking analysis was performed as a preliminary assessment of potential interactions with falcipain-2. However, the absence of correlation between predicted binding affinities and experimental antiplasmodial activity suggests that falcipain-2 inhibition is unlikely to represent the primary mechanism of action. Further studies, including direct enzyme inhibition assays and broader mechanistic investigations, are required to identify the molecular targets responsible for the observed antiplasmodial effects. Overall, these findings provide preliminary pharmacological support for the ethnomedicinal use of *H. barteri* and highlight compound **1** as a moderately active constituent that may serve as a starting point for further optimization. Future investigations should explore additional plant organs and structure–activity relationships to identify other potentially active compounds.

## CRediT authorship contribution statement

**Dé Ndonaï-Koula Lafya Bodeboret Djimtoingar:** Writing – original draft, Validation, Methodology, Investigation, Conceptualization. **Jean Noël Nyemb:** Writing – review & editing, Writing – original draft, Visualization, Validation, Project administration, Methodology, Formal analysis, Data curation, Conceptualization. **Hervé Landry Ketsemen:** Validation, Software, Methodology, Investigation, Data curation. **Joël Abel Gbaweng Yaya:** Validation, Methodology, Investigation. **Roméo Feunaing Toko:** Writing – review & editing, Methodology, Investigation. **Hinlina Yohanna:** Writing – original draft, Data curation. **Samuelson Martin Luther King Boum:** Writing – review & editing, Validation, Formal analysis, Data curation. **Céline Hénoumont:** Software, Resources, Data curation. **Sophie Laurent:** Software, Resources, Formal analysis, Data curation. **Emmanuel Talla:** Supervision. **Marcello Iriti:** Writing – review & editing, Visualization, Validation, Funding acquisition.

## Disclosure statement

No conflict of interest was reported by the authors.

## Funding

This work has been financially supported by the Congolese Foundation for Medical Research via the 2023 edition Program ‘Women and Science’ in partnership with the Bayer Foundation and by the International Evangelic Federation of Cameroonians Fellows (FEAIC) during the Doctoral Scholarship Program 2024 edition.

## Declaration of competing interest

The authors declare that they have no known competing financial interests or personal relationships that could have appeared to influence the work reported in this paper.

## Acknowledgements

The authors are grateful to the French Government Embassy in Chad for the monthly allowance provided via the Cooperation Service of Cultural Action (SCAC) through the Regional Doctoral Scholarship Program 2022 and 2024 edition/Grant N°159613P

## Abbreviations

$^{13}$C NMR: Carbon-13 Nuclear Magnetic Resonance; $^{1}$H NMR: Proton Nuclear Magnetic Resonance; ADT: AutoDock Tools; ANOVA: Analysis of Variance; CC: Column Chromatography; DPPH: 1,1-Diphenyl-2-picrylhydrazyl; ESI-MS: ElectroSpray Ionization Mass Spectrometry; EtOAc: Ethyl Acetate; EtOH: Ethanol; FC: Folin–Ciocalteu; FP2: Falcipain-2; FRAP: Ferric Reducing Antioxidant Power; GAE: Gallic Acid Equivalent; HEPES: 4-(2-Hydroxyethyl)-1-piperazineethanesulfonic acid; $IC_{50}$: Half-Maximal Inhibitory Concentration; MeOH: Methanol; *Pf*3D7: Chloroquine-sensitive strain of *Plasmodium falciparum*; *Pf*Dd2: Multidrug-resistant strain of *Plasmodium falciparum*; RBC: Red Blood Cells; RP: Reducing Power; SYBR: SYBR Green I Fluorescent Dye; TMS: Tetramethylsilane; TLC: Thin Layer Chromatography; TPC: Total Phenolic Content; WHO: World Health Organization; *H. barteri: Haematostaphis barteri*.

## Appendix A. Supplementary data

Supplementary data to this article can be found online at https://doi.org/10.1016/j.jep.2026.121438.

## Data availability

Data will be made available on request.

## References

Abdou, J.P., Nyemb, J.N., Momeni, J., Fadimatou, A., Gbaweng, A.J.Y., Tsopmejio, J.P., et al., 2022. A new cytotoxic ceramide from *Dalbergia boehmii* Taub. stem bark. Pharmacogn. Res. 14 (4), 442–445.

Adekunle, Y.A., Samuel, B.B., Nahar, L., Fatokun, A.A., Sarker, S.D., 2025. Phytosterol glycosides from *Olax subscorpioidea* oliv. Exhibit cytotoxic effects in *in vitro* and *in silico* studies. Pharm. Sci. 31 (3), 294–303. https://doi.org/10.34172/PS.025.40914.

Ahmed, A.O.A., Nkhoma, S.C., Zaman, S., Rashid, S., Bradford, R., Stedman, T.T., Molestina, R.E., 2024. In vitro antimalarial susceptibility profile of Plasmodium falciparum isolates in the BEI Resources repository. Antimicrob. Agents Chemother. 68 (10), e0118923. https://doi.org/10.1128/aac.001189-23.

Arbonnier, M., 2002. *Arbres, Arbustes Et Lianes Des Zones Sèches D'Afrique De L'Ouest* (2$^{E}$ Édition). CIRAD - MNHN.

Batista, R., De Jesus Silva Júnior, A., De Oliveira, A.B., 2009. Plant-derived antimalarial agents: new leads and efficient phytomedicines. Part II. Non-alkaloidal natural products. Molecules 14 (8), 3037–3072.

Boampong, J.N., Karikari, A.A., Ameyaw, E.O., 2015. *In vivo* antiplasmodial and *in vitro* antioxidant properties of stem bark extracts of *Haematostaphis barteri*. Asian Pacific J. Trop. Biomed. 5 (6), 446–450. https://doi.org/10.1016/j.apjtb.2015.02.002.

Dieng, S.I.M., Fall, A.D., Diatta-Badji, K., Sarr, A., Sene, M., Sene, M., et al., 2017. Evaluation de l'activité antioxydante des extraits hydro-ethanoliques des feuilles et écorces de *Piliostigma thonningii* Schumach. Int. J. Biol. Chem. Sci. 11 (2), 768–776.

Djoukeng, J.D., Abou-Mansour, E., Tapondjou, L.A., Lontsi, D., Tabacchi, R., 2007. Identification of ellagic acid derivatives from stem bark of *Syzygium guineense* (Myrtaceae). Nat. Prod. Commun. 2 (3), 261–266.

Dongmo, K.J.J., Tali, M.B.T., Fongang, Y.S.F., Taguimjeu, P.L.K.T., Kagho, D.U.K., Bitchagno, G.T., Lenta, B.N., Boyom, F.F., Sewald, N., Ngouela, S.A., 2023. In vitro antiplasmodial activity and toxicological profile of extracts, fractions and chemical vonstituents of leaves and stem bark from Dacryodes efulis (Burseraceae). BMC Complement. Med. Ther. 23, 211. https://doi.org/10.1186/s12906-023-03957-2.

Ezekiel, J.S., Adamu, H.M., Chindo, I.Y., Garba, I.H., 2016. Phytochemical profile and antioxidant activities of solvent-solvent fractions of *Haematostaphis barteri* hook F. (Anacardiaceae) stem bark extracts. Int. J. Pharmacogn. Phytochem. Res. 8 (1), 51–56.

Happi, G.M., Sikam, K.G., Dietl, A., Reinhardt, J.K., Dzouemo, L.C., Konfor, S.M., Rakhmanov, M., Wansi, J.D., Teufel, R., 2025. Highly oxygenated antiplasmodial and non-hemolytic $\Delta^{7,9(11)}$ stigmastane-type steroids from the twigs of *Vernonia amygdalina* Delile. Phytochem 229, 114286. https://doi.org/10.1016/j.phytochem.2024.114286.

Hatami, T., Sa, E., Ss, M., M, M., 2014. Total phenolic contents and antioxidant activities of different extracts and fractions from the aerial parts of Artemisia biennis willd. IJPR 13 (2). https://pubmed.ncbi.nlm.nih.gov/25237350/.

Heim, K.E., Tagliaferro, A.R., Bobilya, D.J., 2002. Flavonoid antioxidants: chemistry, metabolism and structure-activity relationships. J. Nutr. Biochem. 13 (10), 572–584.

Iheanacho, C., Akubuiro, P.C., Oseghale, I.O., Imieje, V.O., Erharuyi, O., Ogbeide, K., Falodun, A., Jideonwo, A., 2024. Isolation and charactérization of stigmasterol and b- sitosterol fron Anacardium occidentale stem bark (Anacardiaceae): Cashew stem bark. Adv. J. Plant. Biol. 5 (1), 1–15.

Indriani, I., Aminah, N.S., Puspaningsih, N.N.T., 2020. Antiplasmodial activity of stigmastane steroids from Dryobalanops oblongifolia stem bark. Open Chem. 18 (1), 259–264. https://doi.org/10.1515/chem-2020-0027.

Konyanee, A., Chaniad, P., Chukaew, A., et al., 2024. Antiplasmodial potential of isolated xanthones from Mesua ferrea Linn. roots: an *in vitro* and in silico molecular docking and pharmacokinetics study. BMC Complement. Med. Ther. 24, 282. https://doi.org/10.1186/s12906-024-04580-5.

Lambros, C., Vanderberg, J.P., 1979. Synchronization of *Plasmodium falciparum* erythrocytic stages in culture. J. Parasitol. 65, 418. https://doi.org/10.2307/3280287.

Liu, J.C., Wang, H.F., Pei, Y.H., Yu, L.L., 2023. Constituents from cultures of the higher fungus *Pholiota nameko*. Chem. Nat. Compd. 59 (2), 403–405.

Madeleine, D.T., Noël, N.J., de Theodore, A.A., Abdoulaye, H., Talla, E., Laurent, S., et al., 2020. Antioxidant activities and chemical constituents from stem bark of *Ficus abutilifolia*. Miq (Moraceae). EJMP. 31 (13), 48–59.

Mahamat, A., Nyemb, J.N., Gade, I.S., Talka, E., Laurent, S., Mbafor, J.T., 2021. Leptadeniamide, a new ceramide from Leptadenia hastata Pers. (Decne) (Asclepiadeceae) and antimicrobial activity. Int. J. Chem. Sci. 5 (2), 1–5.

Mitchell, J.D., Pell, S.K., Bachelier, J.B., Warschefsky, E.J., Joyce, E.M., Canadell, L.C., da Silva-Luz, C.L., Coiffard, C., 2022. Neotropical Anacardiaceae (cashew family). Bra. J. Bot. 49, 139–180. https://doi.org/10.1007/s40415-022-00793-5.

Mohammed, N., Yaro, A., Balarabe Nazifi, A., 2017. Evaluation of hepatoprotective activity of methanol stem bark extract of *Haematostaphis barteri* Hook. F. against paracetamol and carbon tetrachloride-induced liver injury in rats. AJPT. 6, 88–95.

Muganza, D.M., Fruth, B., Nzunzu, J.L., Tuenter, E., Foubert, K., Cos, P., Maes, L., Cimanga, K., Exarchou, V., Apers, S., Pieters, L., 2016. In vitro antiprotozoal activity and cytotoxicity of extracts and isolated constituents from Greenwayodendron suaveolens. J. Ethnopharmacol. 193, 510–516.

Munvera, A., Nyemb, J.N., Alfred Ngenge, T., Mafo, M.A.F., Nuzhat, S., Nkengfack, A.E., 2021. First report of isolation of antibacterial ceramides from the leaves of *Euclinia longiflora* salisb. Nat. Prod. Commun. 16 (11), 1934578X211048628.

Mvingu, B.K., Mawete, T.D., Kayembe, J.S., Ngbolua, K.-t.-N., Kafuti, Y.S., Mbala, B.M., 2025. Antioxidant and Antiproliferative activities of Root Bark extracts of Lannea Antiscorbutica (Hiern) Engl and isolation of two steroids. J. Clin. Cas. Rep. Med. Image Health Sci. 10 (3), 1–8.

Njinga, N.S., Sule, M.I., Pateh, U.U., Hassan, H.S., Abdullahi, S.T., Ache, R.N., 2016. Isolation and antimicrobial activity of *β*-sitosterol-3-*O*-glucoside from *Lannea kerstingii* engl. & K. Krause (Anacardiacea). JHASNU 6 (1), 4–8.

Nyemb, J.N., Magnibou, M.L., Talla, E., Tchinda, A.T., Tchuenguem, R.T., Henoumont, C., Laurent, S., Mbafor, J.T., 2018. Lipids constituents from *Gardenia aqualla* Stapf & Hutch. Open Chem. 16, 371–376.

Pardo, F., Perich, F., Torres, R., Delle Monache, F., 2000. Stigmast-4-ene-3, 6-dione an unusual phytotoxic sterone from the roots of Echium vulgare L. Biochem. Syst. Ecol. 28 (9), 911–913.

Rice-Evans, C., Miller, N., Paganga, G., 1997. Antioxidant properties of phenolic compounds. Trends Plant Sci. 2 (4), 152–159. https://doi.org/10.1016/S1360-1385(97)01018-2.

Roger, T., Guidawa, F., Bertine, T., Mariette, A., Richard, D., Patrick, S.N., Pierre-Marie, M., 2022. Importance Socioéconomique et Ethnomédicinale de *Haematostaphis barteri* Hook F. dans les Localités de Bidzar, Figuil, Boula-ibbi et Lagam, Nord-Cameroun. ESJ 18 (27). https://doi.org/10.19044/esj.2022.v18n27p227, 227-227.

Schulze-Kaysers, N., Feuereisen, M.M., Schieber, A., 2015. Phenolic compounds in edible species of the Anacardiaceae family - a review. RSC Adv. 5, 73301–73315. https://doi.org/10.1039/C5RA11746A.

Singh, K., Kaur, H., Smith, P., de Kock, C., Chibale, K., Balzarini, J., 2022. Screening of potential antiplasmodial agents targeting cysteine protease-Falcipain 2: a computational pipeline. J. Biomol. Struct. Dyn. 40 (20), 9923–9937.

Smilkstein, M., Sriwilaijaroen, N., Kelly, J.X., Wilairat, P., Riscoe, M., 2004. Simple and inexpensive fluorescence-based technique for high-throughput antimalarial drug screening. Antimicrob. Agents Chemother. 48 (5), 1803–1806. https://doi.org/10.1128/AAC.48.5.1803-1806.2004.

Talla, E., Nyemb, J.N., Tiabou, A.T., Djou, S.G.Z., Biyanzi, P., Sophie, L., Elst, L.V., Tanyi, J.M., 2016. Antioxidant activity and a new ursane-type triterpene from vitellaria paradoxa (Sapotaceae) stem barks. Eur. J. Med. Plants. 16 (3), 1–20.

Trager, W., Jensen, J.B., 1976. Human malaria parasites in continuous culture. Science 193 (4254), 673–675. https://doi.org/10.1126/science.781840.

Vasquez, M., Zuniga, M., Rodriguez, A., 2021. Oxidative stress and pathogenesis in malaria. Front. Cell. Infect. Microbiol. 11, 768182. https://doi.org/10.3389/fcimb.2021.768182.

Wei, K., Li, W., Koike, K., Pei, Y., Chen, Y., Nikaido, T., 2004. Complete $^{1}H$ and $^{13}C$ NMR assignments of two phytosterols from roots of *Piper nigrum*. Magn. Reson. Chem. 42 (3), 355–359.

WHO, 2024. World Malaria Report 2024: Addressing Inequity in the Global Malaria Response. Geneva.consulted on 09/10/2025 at 9: 00 A.M.